

PNNL-32963

LDRD Final Report: Highly Segmented Silicon Strip Detectors for Radiation Detection

June 2022

Todd W Hossbach
Eric D Church
James Fast
Michael F Mayer
Johnathan L Slack

DISCLAIMER

This report was prepared as an account of work sponsored by an agency of the United States Government. Neither the United States Government nor any agency thereof, nor Battelle Memorial Institute, nor any of their employees, makes **any warranty, express or implied, or assumes any legal liability or responsibility for the accuracy, completeness, or usefulness of any information, apparatus, product, or process disclosed, or represents that its use would not infringe privately owned rights.** Reference herein to any specific commercial product, process, or service by trade name, trademark, manufacturer, or otherwise does not necessarily constitute or imply its endorsement, recommendation, or favoring by the United States Government or any agency thereof, or Battelle Memorial Institute. The views and opinions of authors expressed herein do not necessarily state or reflect those of the United States Government or any agency thereof.

PACIFIC NORTHWEST NATIONAL LABORATORY
operated by
BATTELLE
for the
UNITED STATES DEPARTMENT OF ENERGY
under Contract DE-AC05-76RL01830

Printed in the United States of America

Available to DOE and DOE contractors from
the Office of Scientific and Technical Information,
P.O. Box 62, Oak Ridge, TN 37831-0062

www.osti.gov

ph: (865) 576-8401

fox: (865) 576-5728

email: reports@osti.gov

Available to the public from the National Technical Information Service
5301 Shawnee Rd., Alexandria, VA 22312

ph: (800) 553-NTIS (6847)

or (703) 605-6000

email: info@ntis.gov

Online ordering: <http://www.ntis.gov>

LDRD Final Report: Highly Segmented Silicon Strip Detectors for Radiation Detection

June 2022

Todd W Hossbach
Eric D Church
James Fast
Michael F Mayer
Johnathan L Slack

Prepared for
the U.S. Department of Energy
under Contract DE-AC05-76RL01830

Pacific Northwest National Laboratory
Richland, Washington 99354

Abstract

Large area highly segmented silicon strip detectors were investigated for use in applied radiation detection applications. Two ASIC-based readout electronics solutions were tested for compatibility. During the analysis, it was determined that significant computational resources and highly specialized firmware are required to reconstruct the data into a meaningful data stream for generalized spectroscopic performance. Future investment in the technology and careful choice of readout ASIC is expected to demonstrate relevance in measuring high activity samples.

Acknowledgement

This research was supported by the National Security Mission, under the Laboratory Directed Research and Development (LDRD) Program at Pacific Northwest National Laboratory (PNNL). PNNL is a multi-program national laboratory operated for the U.S. Department of Energy (DOE) by Battelle Memorial Institute under Contract No. DE-AC05-76RL01830.

Acronyms and Abbreviations

ADC	Analog to Digital Converter
AFE	Analog Front End
ASIC	Application-specific Integrated Circuit
COF	Chip on Film
EVM	Evaluation Module
FPGA	Field-programmable Gate Array
GUI	Graphical User Interface
LED	Light Emitting Diode
LSB	Least Significant Bit
NaN	Not a Number
PCB	Printed Circuit Board
PIPSBox	Passivated Implanted Planar Silicon Beta Cell
RMS	Root Mean Square
TI	Texas Instruments

Contents

Abstract	ii
Acknowledgement	iii
Acronyms and Abbreviations.....	iv
1.0 Introduction	1
2.0 Equipment.....	2
2.1 Silicon Strip Detector	2
2.2 Texas Instrument ASIC.....	2
2.3 Texas Instrument User Software	4
2.4 Detector box.....	6
3.0 Characterization.....	8
3.1 Detector Response to Optical Stimuli	8
3.2 Detector Stability.....	9
3.3 Electronic Noise	12
3.4 Detector Baseline.....	13
4.0 Radioactive Source Measurements.....	15
5.0 Next Steps	19
6.0 Conclusion	22
7.0 References	23

Figures

Figure 1. Top is the 500 μm thick Silicon strip detector used in this study, bonded to the AFE Chip-on-Flex detector.	1
Figure 2. Texas Instruments AFE2256 Evaluation Module.	3
Figure 3. Close-up of an AFE2256 with attached COF adapter.	3
Figure 4. AFE2256 EVM software configuration page.	4
Figure 5. Example noise analysis plot on the TI GUI.	5
Figure 6. Image of the TI GUI grey scale plot.....	6
Figure 7. Computer rendering of the light-tight box with board platform and clamps.	7
Figure 8. Silicon strips mounted with evaluation board in the light-tight box.	7
Figure 9. Histogram of all 512 channel values and the number of counts in each channel. Only the first 207 strips are connected with every 28th strip disconnected	9
Figure 10. Demonstration of signal drift over time. Baseline LSB values drifted to the right over a period of minutes soon after the board was powered on.	10
Figure 11. Demonstration of time dependence on device noise.	11

Figure 12. Histograms of the sum of all channels for a time trial of the detector from power on to 80 minutes. The silicon was then powered down for 30 minutes, powered back on, and two more measurements recorded.	12
Figure 13. Two-dimensional histogram of silicon channels and the time of measurement. A square wave was injected on the HV line with a period of 256 μ s and an amplitude of 400mV. Integration time was set to 12.8 μ s.	13
Figure 14. Three single channel spectra plotted together.	14
Figure 15. Time domain 2D histogram over 206 channels with no source present.....	15
Figure 16. Time domain 2D histogram over 206 channels with ^{137}Cs source present.	16
Figure 17. Noise peak positions for channels 56 to 60.....	16
Figure 18. Top: Sum of all single channel histograms that were shift corrected. Bottom: All 178 active channels plotted together after shift correction.....	17
Figure 19. Remaining signal after noise subtraction.	18
Figure 20. New PCB with silicon strip detector and bonded ASIC.	19
Figure 21. The improved detector in a box and connected to an FPGA board.	20
Figure 22. A 10 μ Ci sealed ^{241}Am source is used to test the detector response.	20
Figure 23. Using a blue LED, the response of the detector can be probed with higher intensity input than what is possible with the available radioactive sources.	21

1.0 Introduction

Highly segmented silicon strip detectors are widely used in particle physics applications for tracking and event reconstruction. In this LDRD, we examined the extension of this technology to applied radiation detection applications. In particular, a class of large-area (70cm^2) highly segmented (768 strips, 120-micron pitch) 500-micron thick strip detectors were investigated.

Silicon detectors have been used for the detection of radioxenon previously at PNNL (PIPSBox)[1, 2]. The higher energy resolution of silicon when compared to plastic scintillators makes them ideal for identifying the complex signatures of the metastable radioxenons. Highly segmented silicon strip detectors would be well equipped to analyze signatures from complex samples that are either mixed matrix or lack extensive chemical pre-processing (e.g. not just pure xenon).

A trip to Fermilab (FNAL) to collaborate with experts in silicon (Si) strip detectors was undertaken to identify a usable sensor with which to begin our research with these detectors. After investigating several sensors at the FNAL Si facility for good behavior with respect to full depletion and breakdown, the sensor in Figure 1 was identified as suitable. FNAL technicians wire-bonded our chosen sensor pads to the Texas Instruments (TI) AFE Chip-on-flex (COF) ASIC continuous readout solution [3]. The sensor-strip pitch, as seen in Figure 1, does not match that of the COF, so roughly every seventh COF strip is left unconnected to the sensor. Some strips at one end of the detector are also not instrumented.

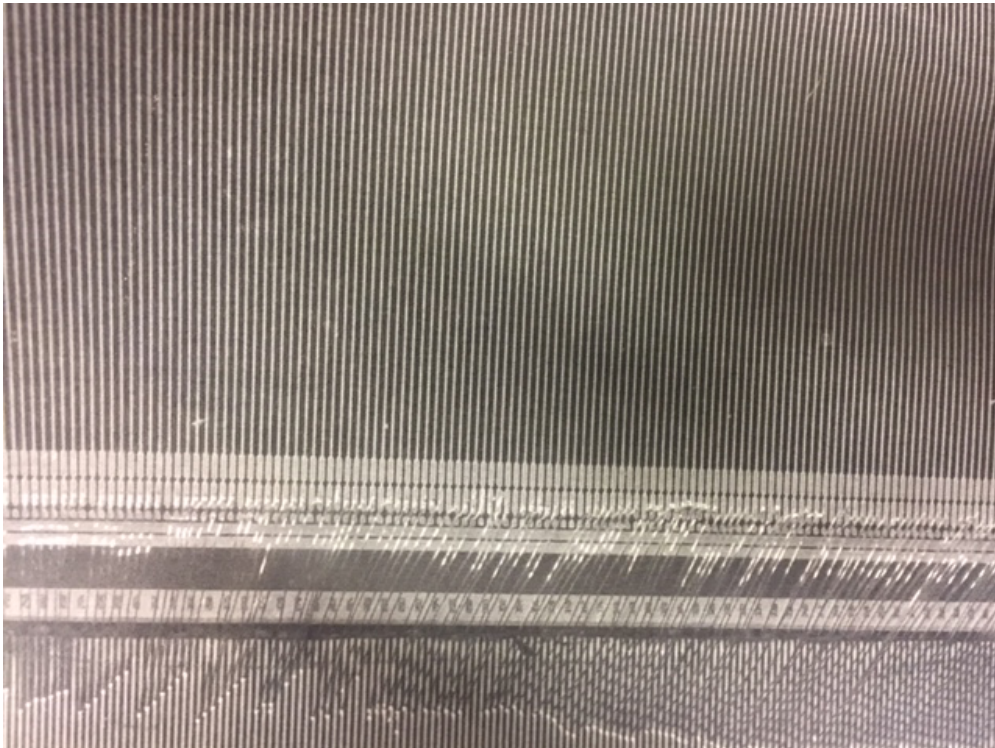


Figure 1. Top is the 500 μm thick Silicon strip detector used in this study, bonded to the AFE Chip-on-Flex detector.

2.0 Equipment

2.1 Silicon Strip Detector

Results from the PIPSBox show that using silicon as a radioxenon detector is feasible. The PIPSBox is a single monolithic piece of silicon 500 μm thick designed for beta and conversion electron spectroscopy of gaseous samples. This is a common thickness for silicon manufacturing and is the same as the silicon strip detector under investigation in this LDRD. The silicon strip detector used in this preliminary setup is segmented into 768 parallel strips with 120-micron pitch and total active area of $\sim 70\text{cm}^2$.

2.2 Texas Instrument ASIC

The Texas Instrument ASIC, Figure 2, consists of two AFE COF cards that slot into two Samtec™ ports on the evaluation module. The AFE2256 is designed to meet the requirements of flat-panel detector x-ray imaging systems with an on-chip 16-bit Analog-to-Digital Converter (ADC) as well as 256 integration channels. As such when the ASIC is collecting data the system runs in a continuous mode and is not triggered on either an internal or external signal. After the set integration time the data is read out in serial across all channels.

The board is powered by a 6 Volt, 3 Amp, low noise power supply and has a low noise reference generator to provide reference voltage to the four DAC's. Each COF can be read simultaneously and come pre-installed with a heatsink clip and thermal pad as shown in Figure 3. An onboard FPGA provides the necessary conversion of the data from the AFE COF's to the USB2.0/3.0 PC output. The module is also equipped with pipeline integration that allows for real time monitoring of data collection [3].

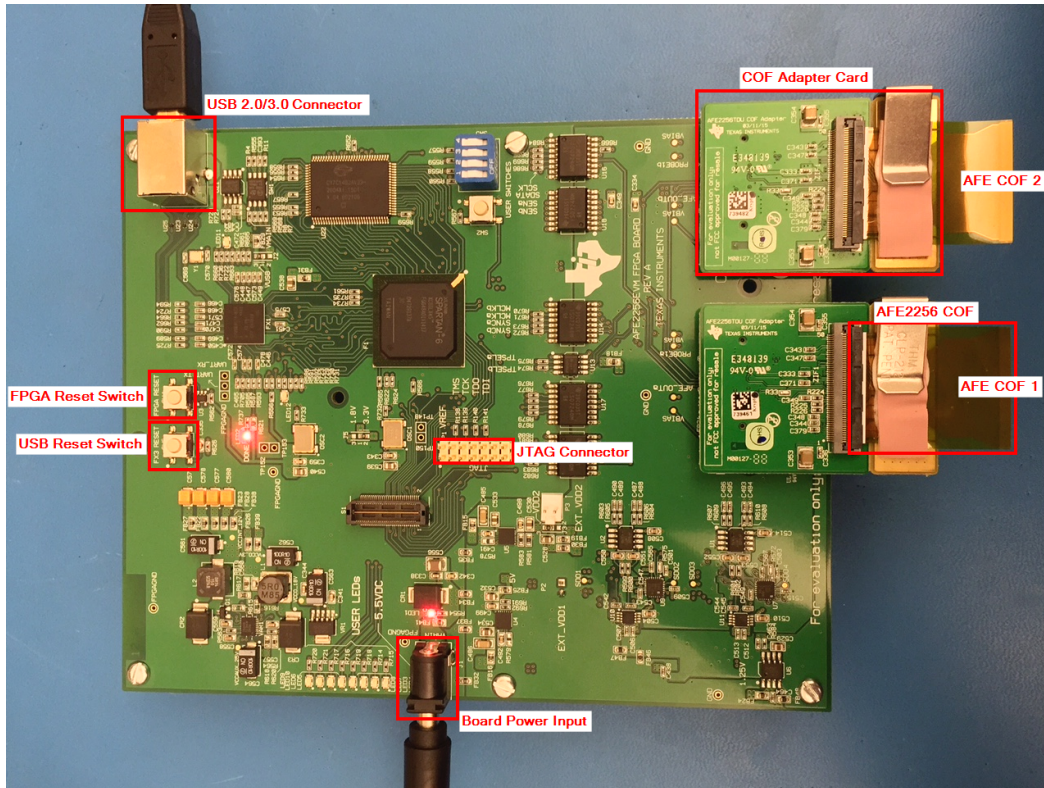


Figure 2. Texas Instruments AFE2256 Evaluation Module.

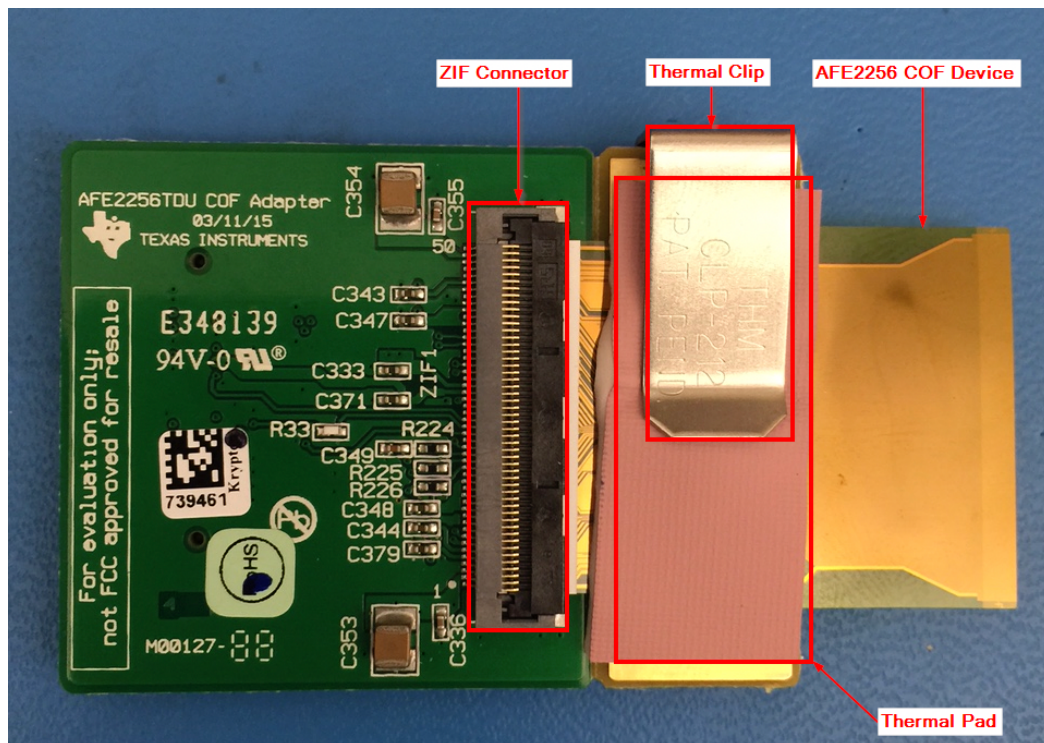


Figure 3. Close-up of an AFE2256 with attached COF adapter.

2.3 Texas Instrument User Software

The AFE2256 came with Texas Instrument software that controlled and read out the device [4]. It can alter several parameters including six input ranges from 0.6pC to 9.6pC, scan times from 12.8µs to 204.8µs, and a low-correlated noise power mode as shown in Figure 4. Granular control of each input channel is possible with user written configuration files. TI provides several config files out of the box to match common client needs. Data from a collection run can be saved in a text format with either raw least significant bit (LSB) values or LSB values with the offset removed. When selecting the remove offset option, the average value of each channel is calculated and then subtracted from every data point in that channel. This provides a method for zeroing the data value scale for each individual channel.

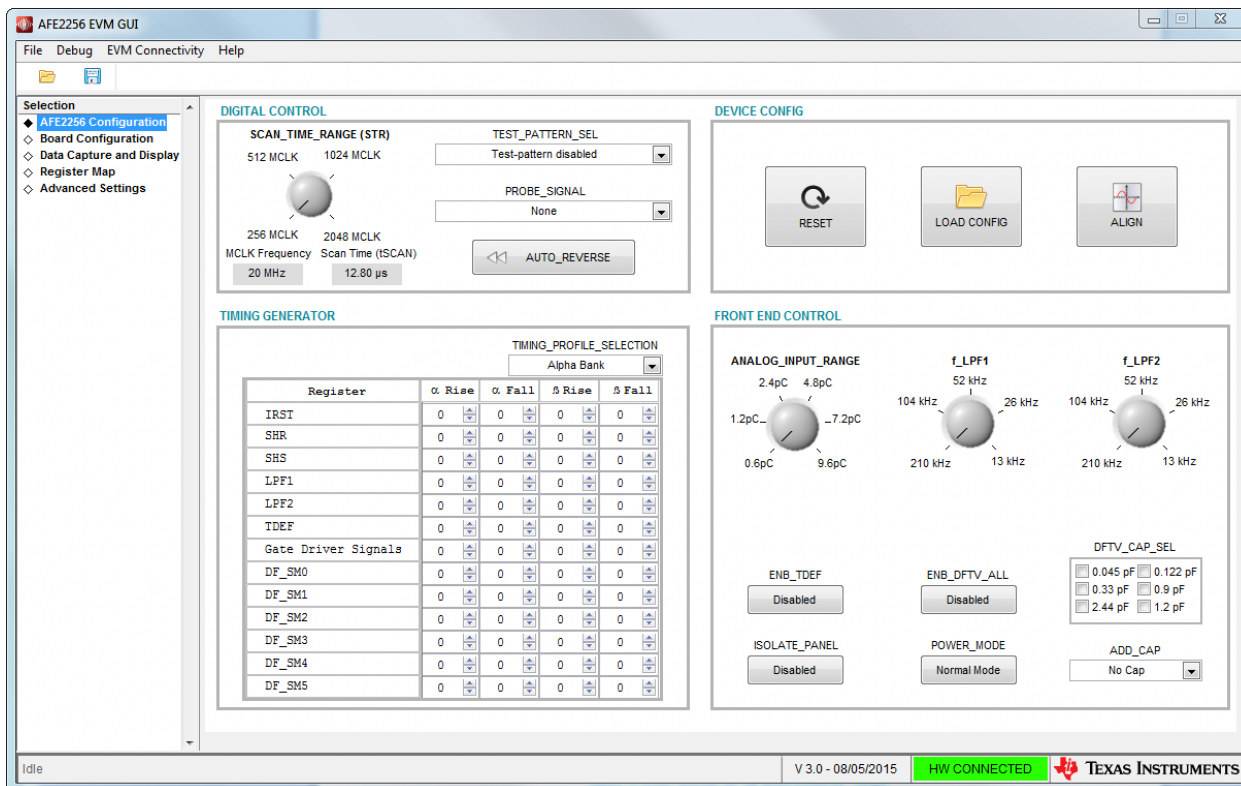


Figure 4. AFE2256 EVM software configuration page.

When capture is selected on the graphical user interface (GUI) the device data is recorded in a text file. The number of text files written corresponds to the number of capture counts selected. The possible number of captures ranges from 1-32 with each file containing LSB values for each of the 512 channels available in a single row for each time the device is read out. Each capture count text file has 768 columns. Therefore, the maximum number of recorded events for a single channel with continuous operation is 24,576.

The TI software has a number of ways to display captured data in real time. The default when selecting the Data Capture and Display tab is the Noise Analysis graph which plots the channel number against the output noise of each channel for a single capture, Figure 5. The output

noise is computed by analyzing a single channel's 768 data points during each capture. Output noise is the only plot that allows the user to change the data displayed from ADC output codes to electron noise.

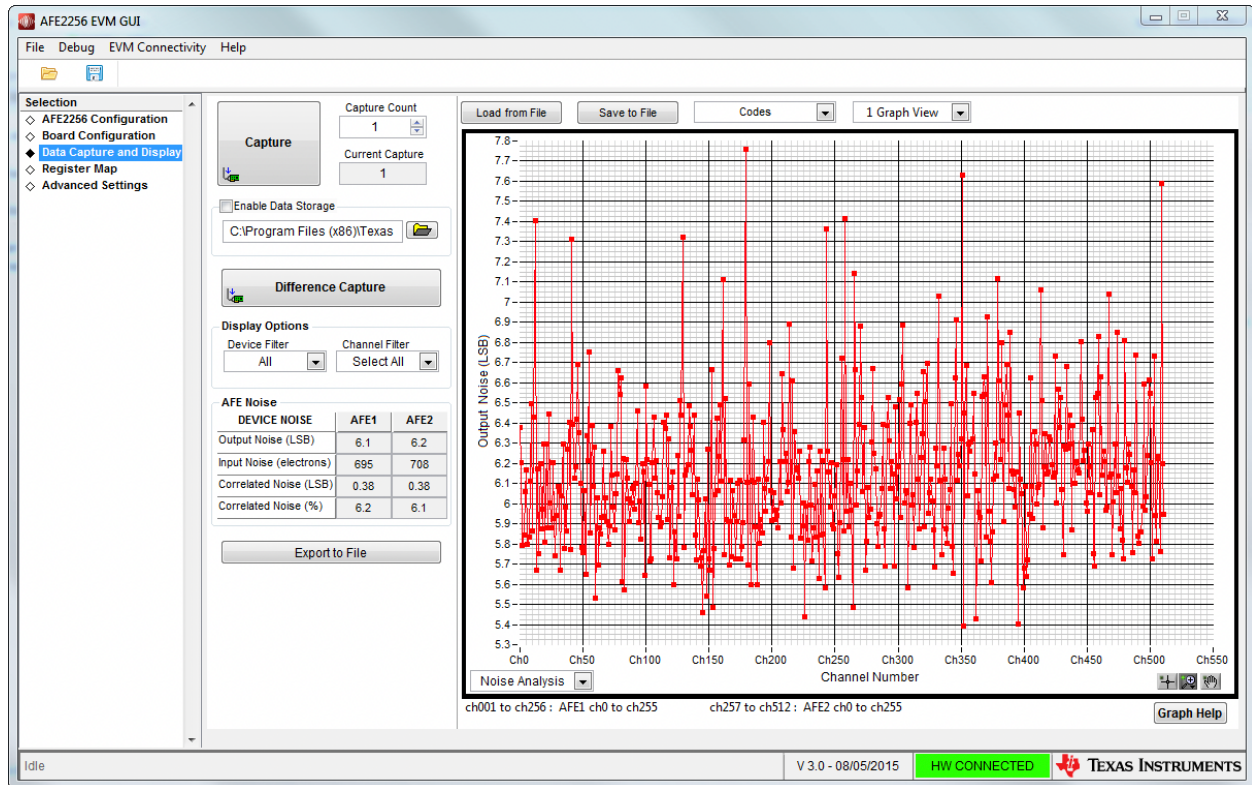


Figure 5. Example noise analysis plot on the TI GUI.

The same data is selected for analysis when the candlestick plot is chosen for display. The candlestick plot shows the mean, minimum, and maximum LSB values for both AFE's and both banks A and B. Individual channels or banks of channels can be filtered out from the plots.

There are two other options for displaying single channel data, the time domain and histogram plots. The time domain plot is simply a measurement number vs output code in LSB's. Channel statistics like the average, Root-Mean-Square (RMS), min, and max are also given. The histogram plot is a simple, configurable, histogram of a file's capture data for a single channel.

Figure 6 displays the last plot type that comes with the TI GUI, the greyscale plot. This is meant for on-the-fly image quality analysis. It maps the two sets of AFE channel's LSB values against the row number of the capture file, functioning like a 2D time histogram for all channels. It includes an option for removing the offset. In practice the remove offset option helps normalize each channel and clean up the noise.

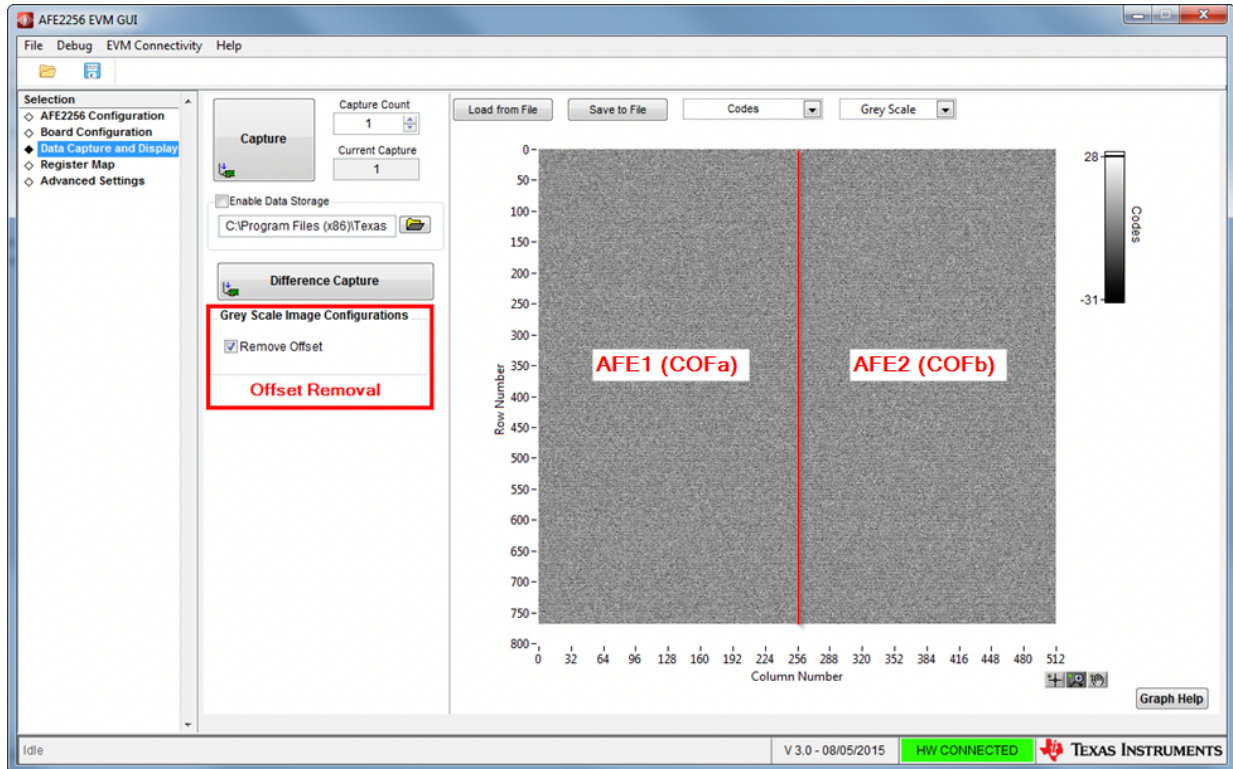


Figure 6. Image of the TI GUI grey scale plot.

2.4 Detector box

Silicon is known to be sensitive to optical photons, so a light-tight box was designed and constructed at PNNL to house the strip detector and wire bonded ASIC boards, see Figure 7. All passthroughs and the feet of the device were sealed to prevent light leakage into the box. The lid was similarly treated with a ¼” wide weatherproof gasket to ensure a light-tight container.

A stable platform was necessary to secure the board in place and properly ground the entire apparatus to avoid static discharge. The evaluation board was secured to an aluminum plate with one inch long, plastic, standoff screws. This was how the detector was received from FNAL. The aluminum plate was held in place in the box with four C-type screw clamps that were in turn secured to a plastic (type) platform on the bottom of the enclosure. Figure 8 is a picture of the system mounted inside the light-tight box. The disconnected AFE chip is in the foreground with white electrical tape holding it in place. Both AFE’s had to be securely plugged into the TI board for the software to boot correctly.

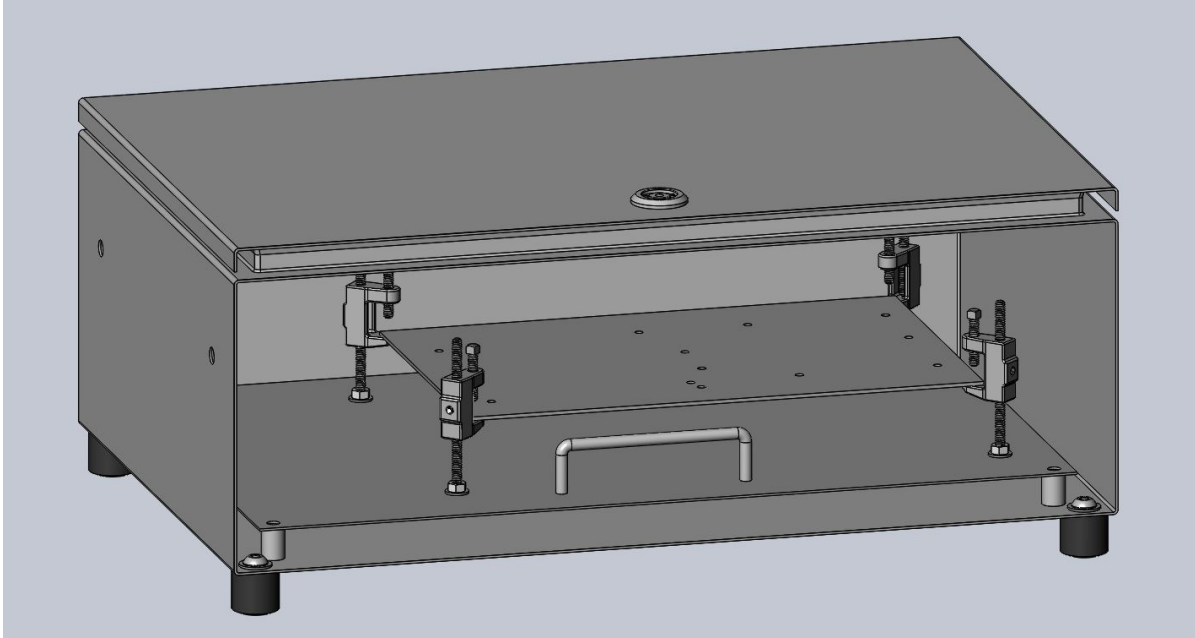


Figure 7. Computer rendering of the light-tight box with board platform and clamps.

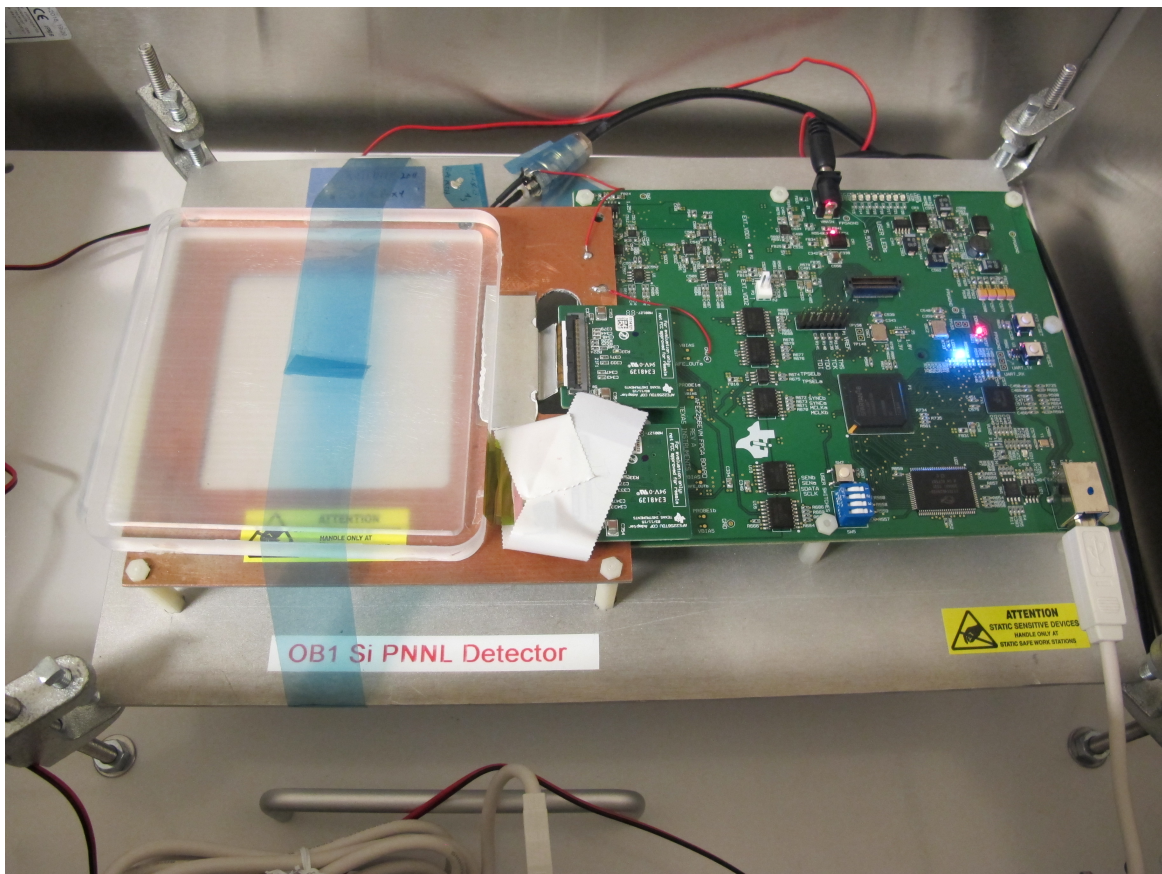


Figure 8. Silicon strips mounted with evaluation board in the light-tight box.

3.0 Characterization

Initial testing with the detector was intended to characterize the device. The limits of the system and its controls were unknown when the device was received. Considerable time was spent adjusting the device, its environment, and the settings on the data collection software. Basic analysis was performed by examining the output of the TI GUI in real time, but a more detailed analysis was performed by analyzing the output text files. These files were analyzed using the ROOT framework to produce histograms for basic spectroscopy by looking at individual channels and channel summing.

3.1 Detector Response to Optical Stimuli

The device arrived from Fermilab before the light-tight box was completed. It was placed on a lab bench and covered by a blackout cloth for initial testing. It was noted almost immediately that when the blackout cover was lifted, and the silicon was exposed to room light, the LSB values graphed by the TI GUI and the current from the HV supply rose rapidly. This indicated the silicon was correctly wired to the ASIC system.

The TI board's output plots cannot be saved. They also only display one collection file at a time in series during the collection period. This makes the GUI useful for on-the-fly adjustments of evaluation board parameters when a clear image or result is expected. When attempting to characterize an unknown device, as in the case of the silicon strip detector, the temporary nature of the GUI plots was not advantageous. Post-processing of collected data was essential.

Figure 9 is a histogram of all available channels on the evaluation board. This run was performed with the system sitting on the lab bench. The horizontal axis is the channel number, and the vertical axis is the sum of the LSB values for each channel during a run of 32 collections. This figure is an example of how the disconnected channels manifested in the data. Wire bonding to the silicon only occurs for the first 206 channels. All channels above that register disconnected or open-contact noise. Within the range 0-206 there are 28 channels that are also disconnected. These manifest graphically as channels with zero LSB value.

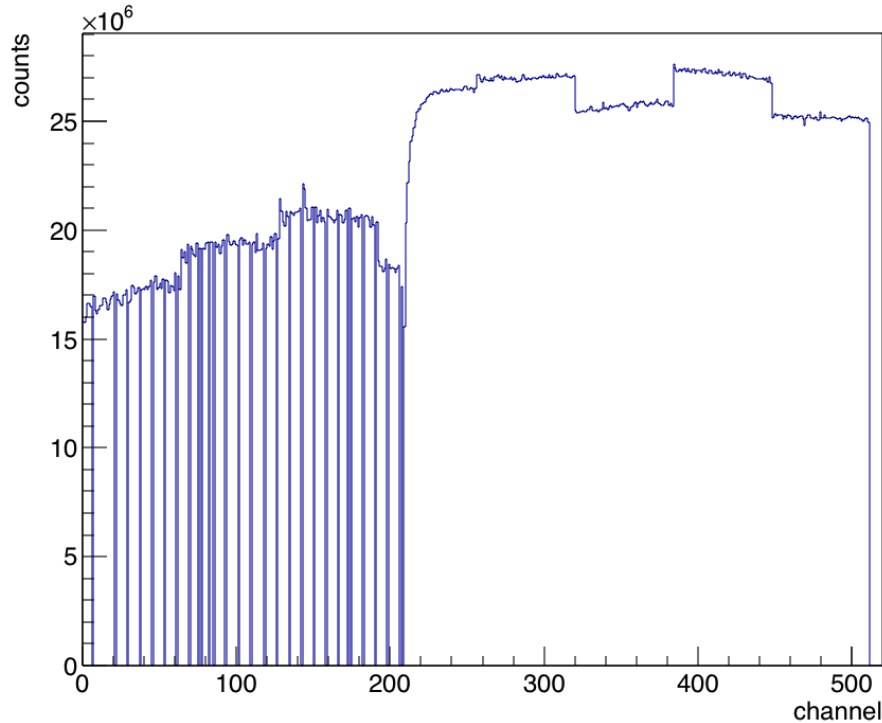


Figure 9. Histogram of all 512 channel values and the number of counts in each channel. Only the first 207 strips are connected with every 28th strip disconnected

3.2 Detector Stability

Stability testing of the system began with the light-tight box. While taking background data a time-dependent drift was noticed. Figure 10 shows a room background spectrum, followed by an ^{241}Am measurement, and a follow up post-sample background measurement. Each set of displayed data is the sum of the first 206 channel histograms for the entire run of 32 collections. The figure demonstrates the drift inherent in the detector system. Time between measurements was approximately two minutes as the high voltage was ramped down, the box briefly opened to insert or remove the source, and time for the high voltage to ramp back up.

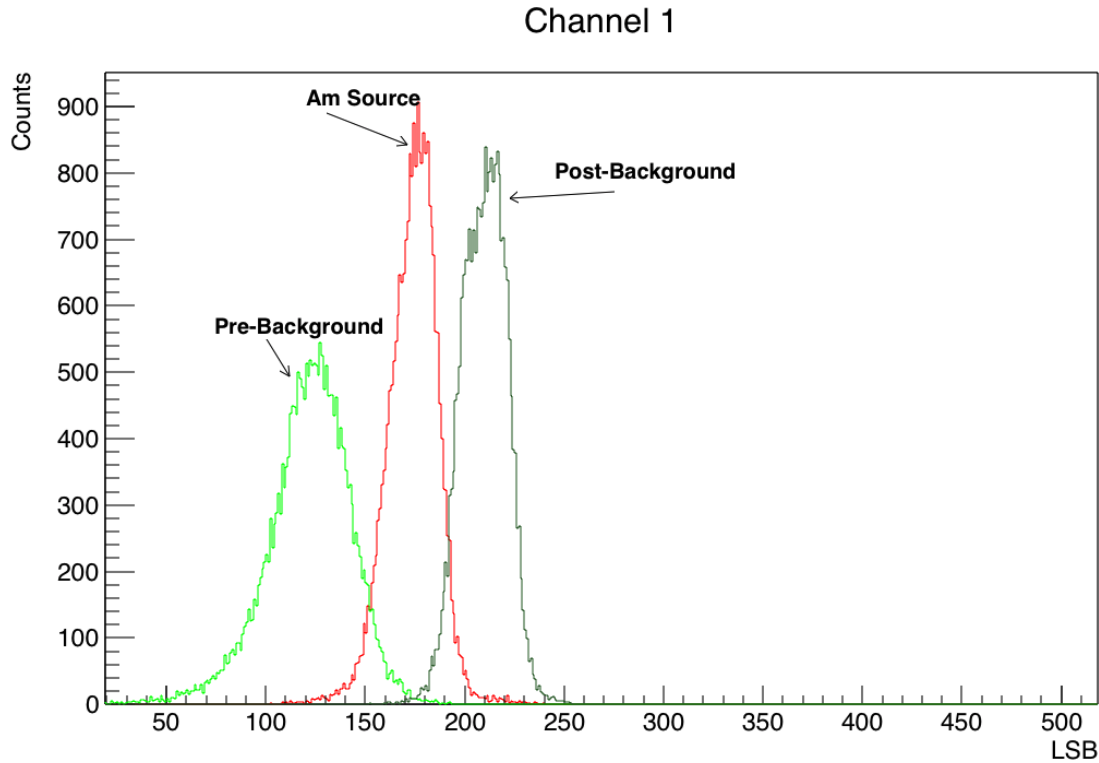


Figure 10. Demonstration of signal drift over time. Baseline LSB values drifted to the right over a period of minutes soon after the board was powered on.

Figure 11 shows the LSB sums in the first 206 channels for a series of background runs. The time that each run was started is marked in the right and delineated on the histograms by varying shades of blue lines. It shows that the total activity on the system increased with time from a low of 5 million counts in a channel to approximately 6 million counts. The change is not linear in time however and suggests the possibility that an equilibrium point may exist. This test was performed with the detector still on the lab bench.

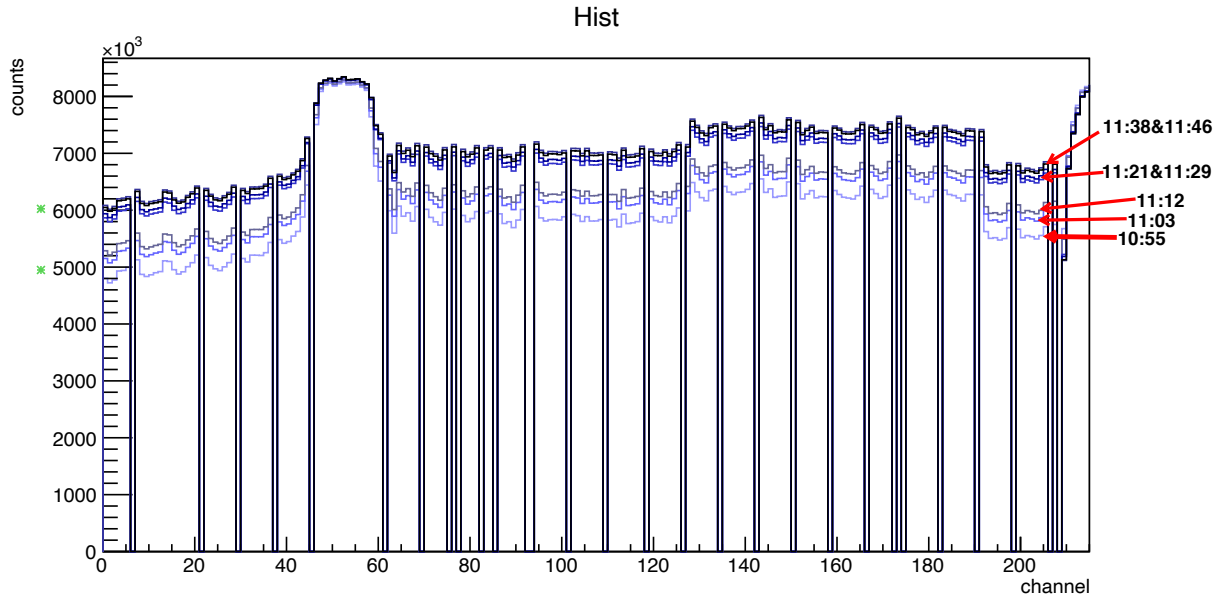


Figure 11. Demonstration of time dependence on device noise.

Figure 12 shows a dedicated stability trial of the system performed shortly after the signal drift was noted. By overlaying the summed channel spectrum for multiple runs a time-dependence on the detector spectra was constructed. All runs were performed for the maximum number of collections. The system was powered on, and then periodic data collections were performed at 10 minutes, 20 minutes, 49 minutes, and 80 minutes. Then the high voltage was shut down for 30 minutes, turned back on, and two more measurements performed (lines 'Power off – 30 min' and 'power up – 10 min'). This test was intended to identify if the silicon strips or the TI board had a “warm-up” time and how long it took to reach an equilibrium. As this figure shows, the shape of the distribution did not reset with just the HV to the silicon turned off, suggesting that the TI board may have some time dependence associated with it, not the silicon strips.

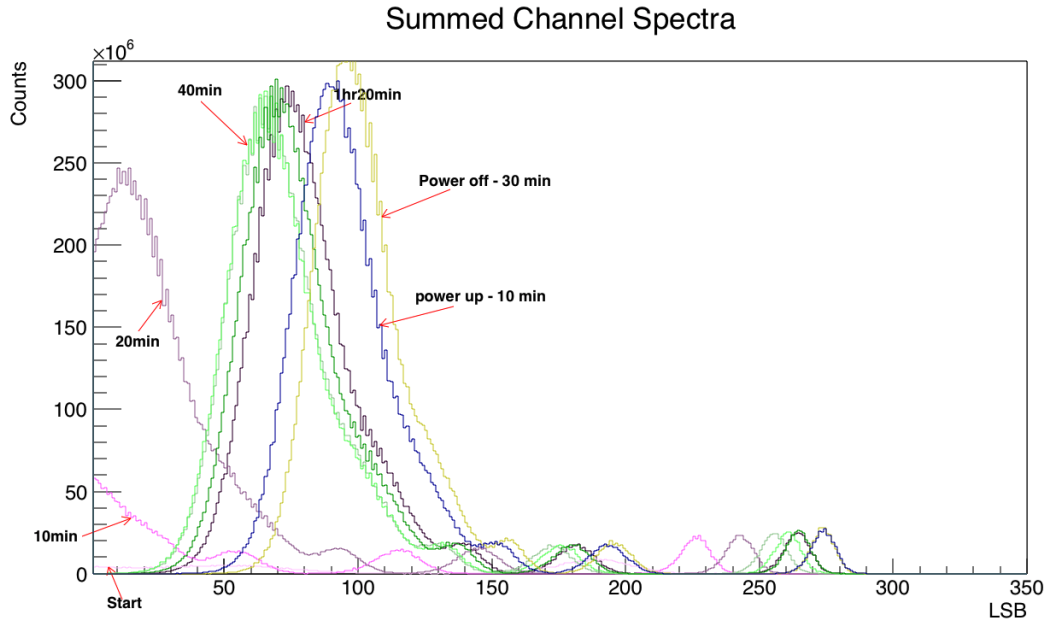


Figure 12. Histograms of the sum of all channels for a time trial of the detector from power on to 80 minutes. The silicon was then powered down for 30 minutes, powered back on, and two more measurements recorded.

A temperature probe was added to the setup and multiple experiments were conducted to find a correlation between the observed drift of the TI board with the temperature at different locations in the light-tight box. No correlation was found at the outer edges of the box, near the silicon, or next to the TI board. The temperature inside the box at all locations tracked directly with the temperature in the lab. There was a correlation found between the warm-up drift of the detector and the current on the HV power supply.

The TI board needed to be powered on for at least two hours before an equilibrium was reached. Data acquisition could then be performed with the minimal amount of drift when the high voltage power supply current measured between 2.8-3.0 μA . Even under these conditions the drift would cause some misalignment between the background run and the source run despite the time between measurements being only on the order of minutes.

3.3 Electronic Noise

The TI ASIC is a continuously operating system with limited data collection intervals due to its intended purpose of being implemented in an x-ray imaging system. It simply collects the accrued charge over an integration time and outputs that charge from the ADC as a LSB. This causes significant noise to be accumulated. Typically, in a silicon strip device used for charged particle or cosmic ray detection there are external detectors that are used to trigger the readout on the silicon, reducing the noise by nearly eliminating unnecessary data collection.

Attempting to reduce the background noise by increasing the statistics with multiple runs of the detector is limited because of the drift in the TI board. Gains made by increased counting statistics of a higher activity source are obscured by subsequent measurements as the noise drifts over the signal area.

3.4 Detector Baseline

All out-of-the-box configuration files from TI provided a zero baseline that assumes positive charge injection coming from any wired detector. This was discovered during work performed with a pulse generator. When a negative edge of the generator was received by the ASIC, the LSB values recorded were either zero or not-a-number (NaN). This led to gaps in the 2D histograms where positive edges could be clearly identified with dead space where the negative edges of the pulse were received.

Figure 13 is a 2D time domain histogram of the first 206 channels. White space is representative of zero or NaN values in the raw data files. Time in this plot proceeds from bottom to top. This figure shows that when a leading square wave edge is positive the detector correctly registers a large increase in LSB value followed by a decay. When the corresponding negative edge impinges on the detector the LSB values are pinned at zero.

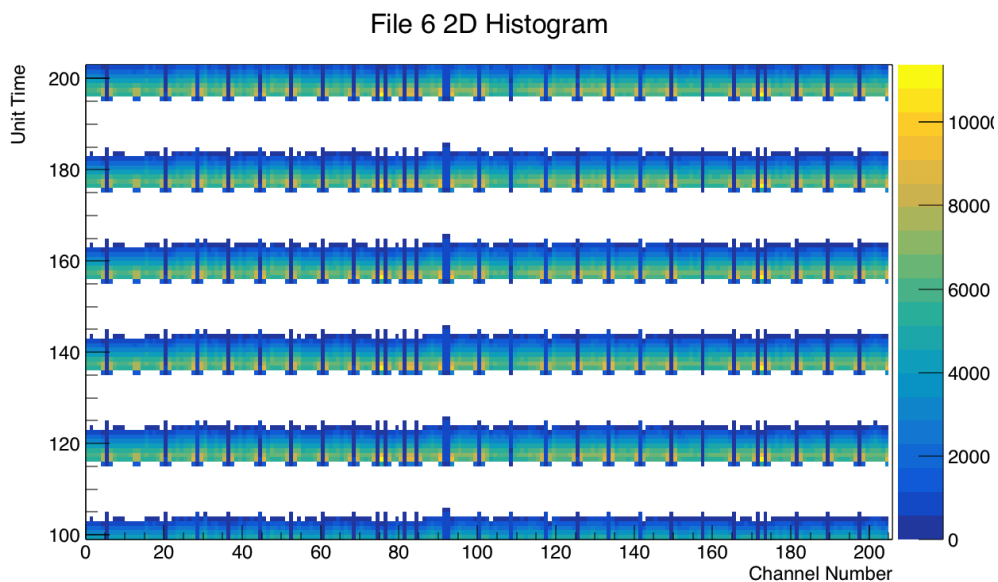


Figure 13. Two-dimensional histogram of silicon channels and the time of measurement. A square wave was injected on the HV line with a period of $256\mu\text{s}$ and an amplitude of 400mV . Integration time was set to $12.8\mu\text{s}$.

Multiple attempts were made to find the right combinations of settings that would raise the zero value from its current position to a reasonable position in the middle of the LSB range. The documentation that came with the TI software did not indicate any direct way to make this change and ultimately a consultation with a TI technician was necessary.

Charge injection tests were conducted to supplement the studies from radioactive sources. In these tests a capacitor, in series with the high voltage connection to the back of the silicon, was pulsed to inject charge on the Si readout strips. Similar tests were conducted using an LED (light emitting diode) instead of delivering a pulse along the high voltage line. An LED is foreseen to be a useful external trigger for subsequent detector development, as its brightness may be varied, the width of the pulse varied, and the LED's location with respect to individual strips may also be scanned.

An individual channel offset was also observed. No silicon strip has the exact same capacitance as another so there is a slight offset to the noise peaks from channel to channel. Figure 14 is an example of the offset inherent in the detector. Single channel histograms for channels 40, 41, and 42 are plotted together. No radioactive source is present. The noise peaks for each channel are offset from each other by seemingly random amounts. Direct summing of channel histograms in this case will likely result in any small signal from the radioactive source being washed out.

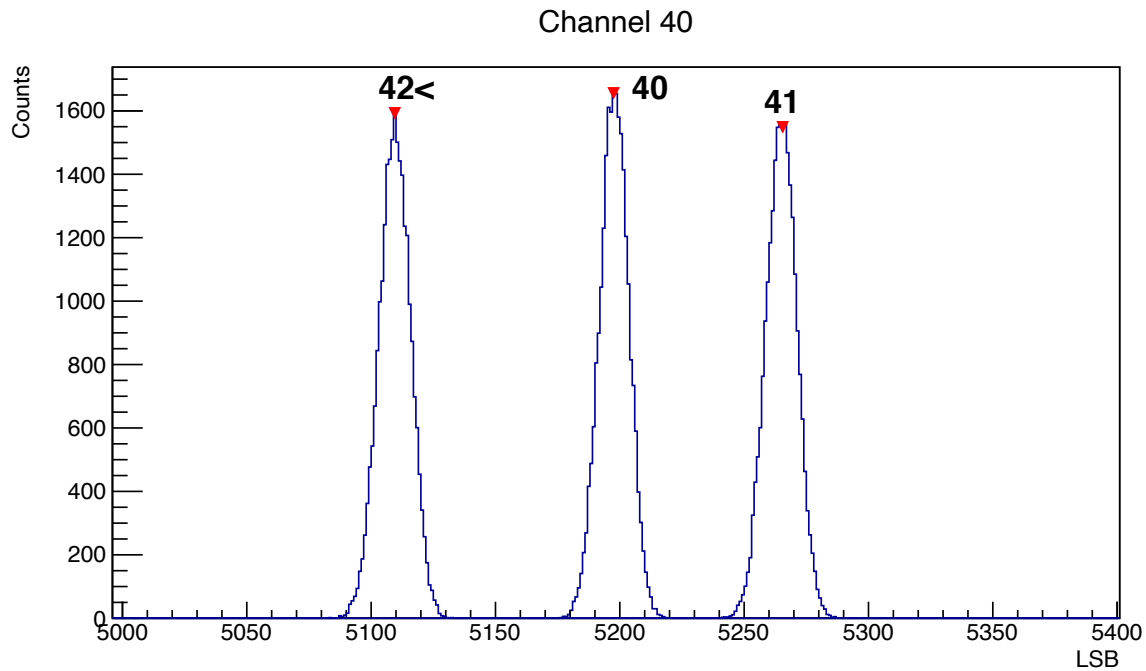


Figure 14. Three single channel spectra plotted together.

4.0 Radioactive Source Measurements

Sealed beta sources were not available during large portions of this research. As a stand-in, a high-activity sealed X-ray source was used – ^{137}Cs . A rough calculation shows that a 100 μCi source of 30 keV X-rays travelling through a few-hundred-micron thick piece of silicon is expected to interact with one of our detector strips roughly 0.1% of the time in the un-triggered 100 microsec sampling windows. The expected 6 fC depositions at the nominal gain setting corresponds to a 50 ADC count shift to the left of the background noise peak.

After consultation with TI tech support, a custom configuration file was developed that successfully moved the measurement baseline and configured the ASIC to be as sensitive as possible to a radioactive source and the resulting holes that move to the positively biased back side of the silicon. Placing a 100 μCi ^{137}Cs source in front of the detector there were clear differences between background and source. Figure 15 and Figure 16 shows 2D time domain histograms of both runs. In the second figure hits of 30-keV X-rays are distinguishable by the large negative values. This is consistent with the predicted negative biasing on the silicon. This confirmed that the silicon strip could absorb the 30-keV X-rays coming from a ^{137}Cs source. Both images were created using the same “remove offset” technique of the TI software.

File 10 2D Histogram

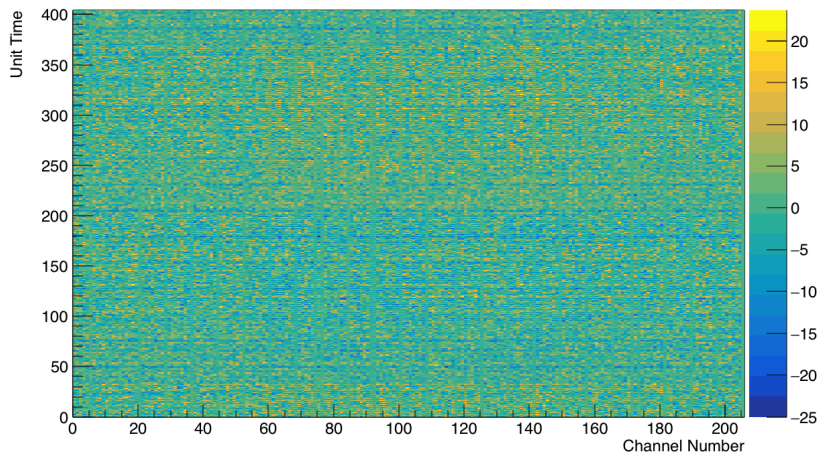


Figure 15. Time domain 2D histogram over 206 channels with no source present.

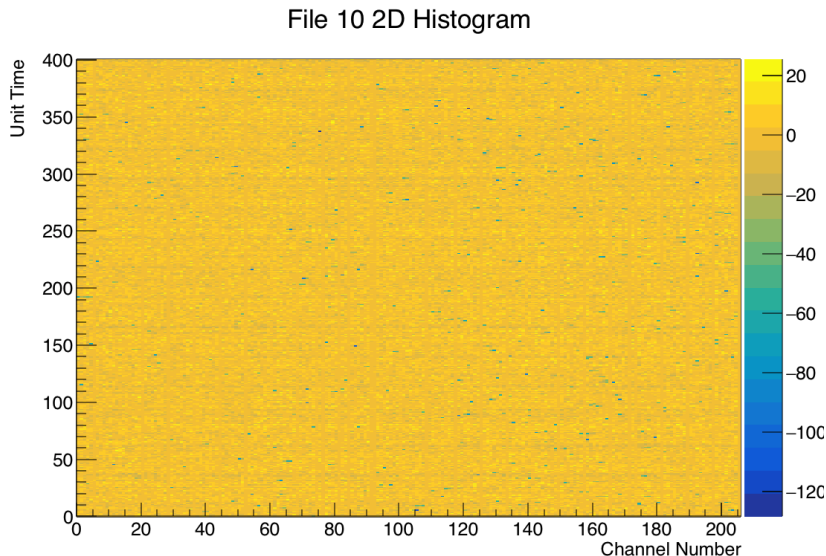


Figure 16. Time domain 2D histogram over 206 channels with ¹³⁷Cs source present.

As discussed earlier there is a unique channel offset for every silicon channel. Figure 17 has channels 56-60 plotted on the same chart. As before, each noise peak for each channel is located at a different position. Each channel also has a left tail from absorption of activity from the ¹³⁷Cs source. No single channel has enough event counts in the region of interest therefore summing was necessary. The noise, due to a lack of triggering, also causes the noise peaks to be orders-of-magnitude larger than the signal counts.

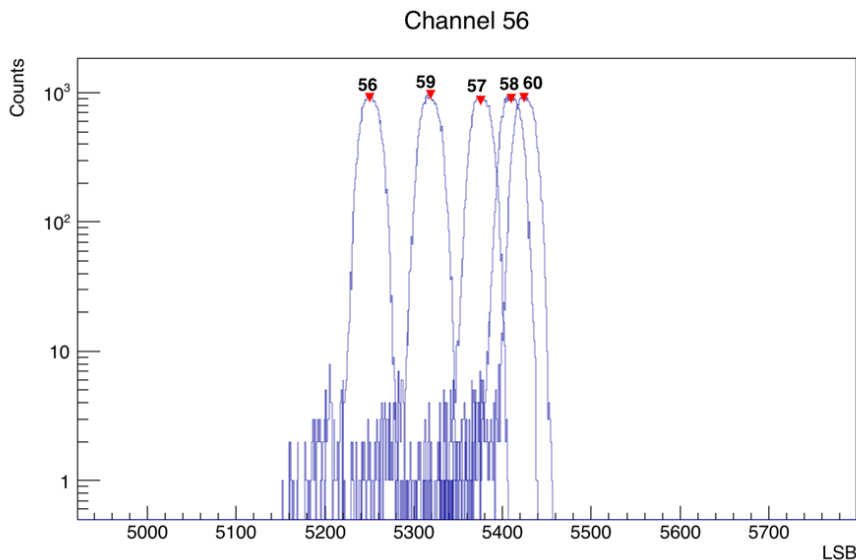


Figure 17. Noise peak positions for channels 56 to 60.

To compensate for the different peak positions, a gaussian peak finding algorithm from ROOT was utilized. Once all peaks were found, each channel histogram was shifted to the same arbitrary position (6000 LSB) to line up every channel peak. The result of which can be seen in the bottom half of Figure 18. Then all 178 connected channels were summed to create an equivalent single histogram as shown in Figure 18 Top. Integrating over the central region and estimating the LSB positions of the region of interest, the noise could be isolated from the signal

counts. This yielded 26,403 counts in the signal region with a signal to noise of approximately 0.6%. This is close to the predicted value of 1% for a 100 μCi ^{137}Cs button source.

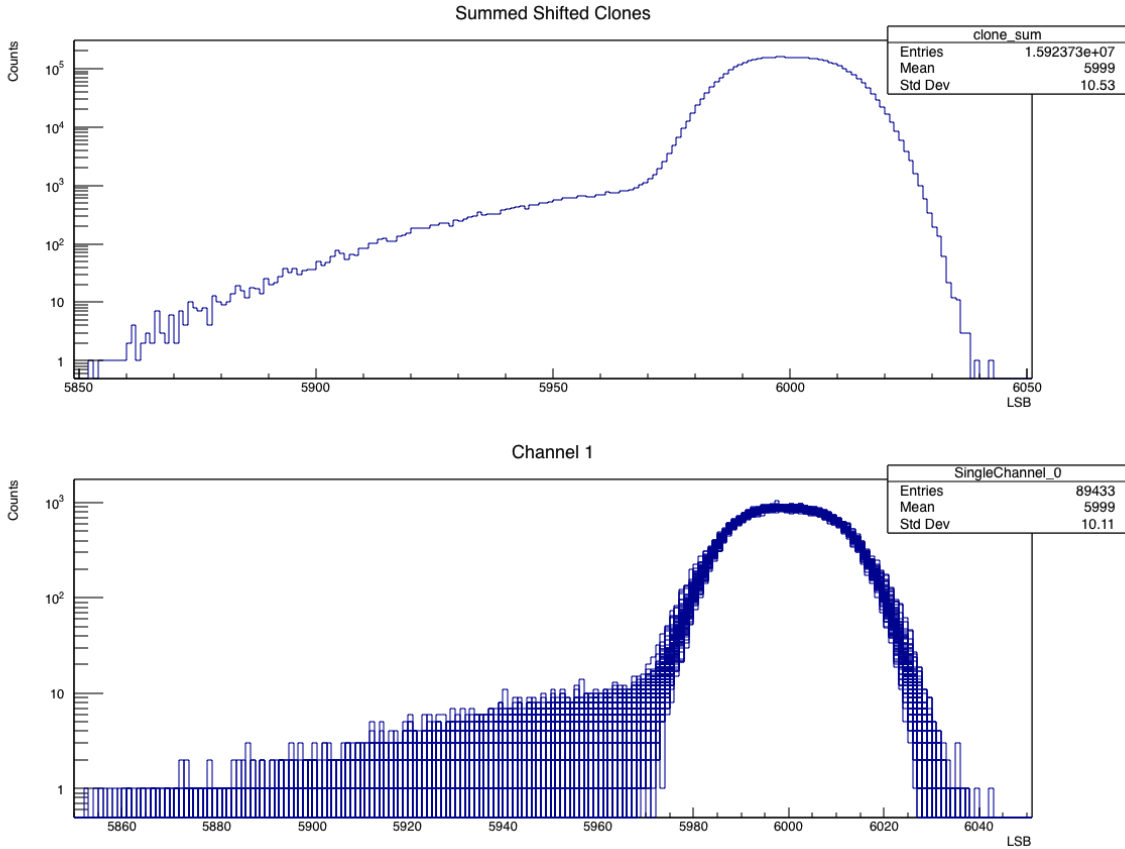


Figure 18. Top: Sum of all single channel histograms that were shift corrected. Bottom: All 178 active channels plotted together after shift correction.

Figure 19 shows the residual signal histogram after the symmetric right-side region of the noise was subtracted off. This histogram has a mean value of 5947 while the original summed channel histogram, Figure 18 Top, had a mean of 5999. The total shift from the central noise to the signal was 52 LSB. This is very nearly the predicted shift of 50 ADC counts.

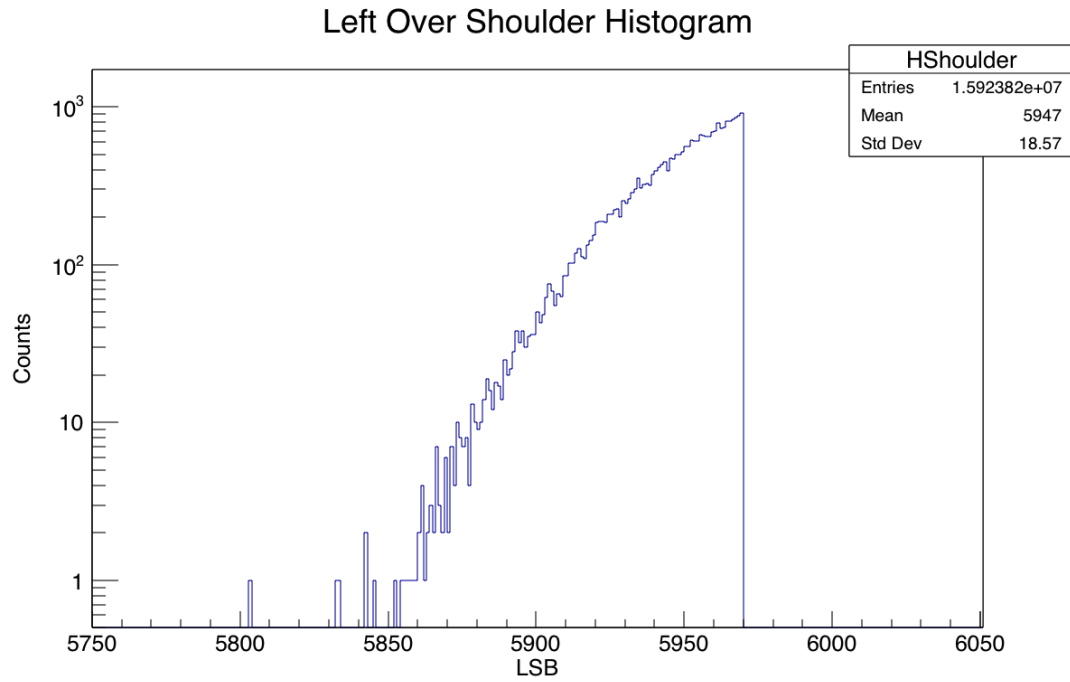


Figure 19. Remaining signal after noise subtraction.

5.0 Next Steps

To address the shortcoming of the continuous readout solution provided by the TI ASIC, a new self-triggered ASIC readout was identified at Fermilab – Skiroc2. A newly designed Printed Circuit Board (PCB) was designed and fabricated as well as the other necessary components. The first boards were populated, and wire bonded to a new silicon strip detector, see Figure 20. A total of three detector systems (silicon sensor, ASICS, and readout electronics) were assembled at Fermilab, see Figure 21. This new detector system promises to improve on several areas where the TI ASIC was sub-optimum. With this new system it will be possible to implement custom triggering. This should drastically improve the signal to noise well above the current <1% range. It will also be possible to define data recording time parameters for minutes- or hours-long collections. Initial testing of the Skiroc2s with radioactive sources and LEDs, see Figure 22 and Figure 23, revealed a defect in the readout boards. By the end of the LDRD project, a solution was identified and the parts were returned to the manufacturer for repair. No further data was obtained with this ASIC by the end of the project.



Figure 20. New PCB with silicon strip detector and bonded ASIC.



Figure 21. The improved detector in a box and connected to an FPGA board.

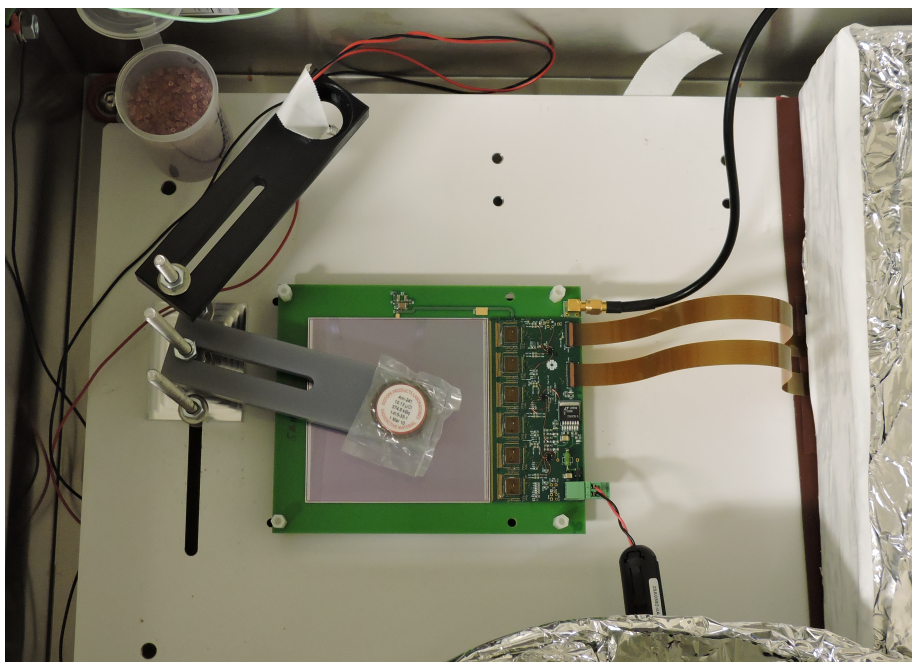


Figure 22. A 10 μCi sealed ^{241}Am source is used to test the detector response.

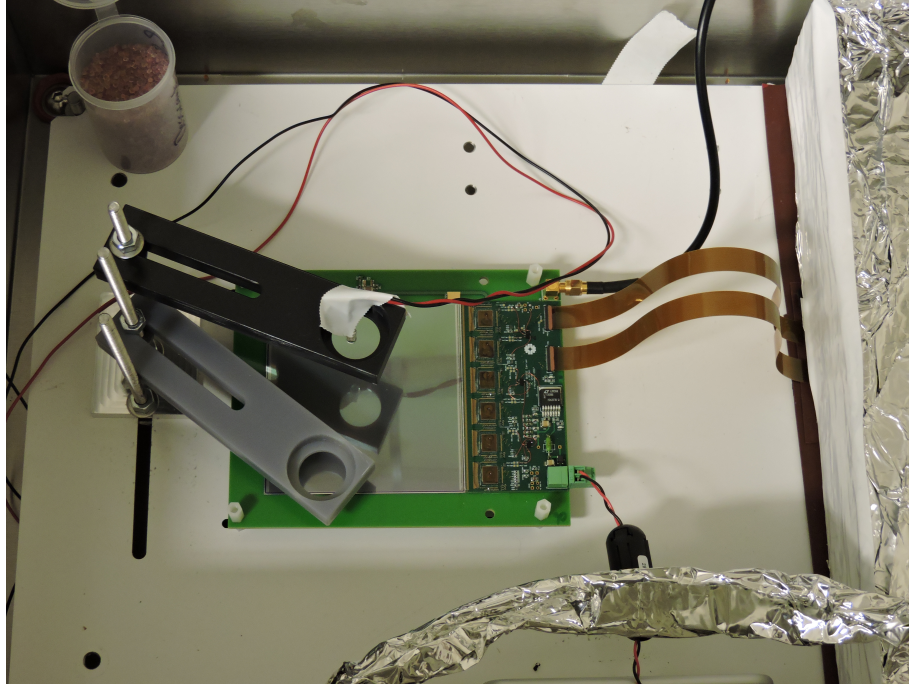


Figure 23. Using a blue LED, the response of the detector can be probed with higher intensity input than what is possible with the available radioactive sources.

6.0 Conclusion

A silicon strip detector, instrumented with a custom Texas Instruments (TI) readout ASIC, successfully measured a ^{137}Cs sealed button source. It was possible to image where and when the X-rays deposited their energy within individual strips. An LED was used to probe the strips and was shown to be a useful calibration tool and external trigger. The baseline electronic noise dominated the data stream because of the inability to trigger the readout. For applied radiation detection, this characteristic along with several other shortcomings of the TI solution, motivated a search of a more optimal solution. An improved ASIC, the Skiroc2, was identified that addressed several improvements over the TI solution – better signal to noise, improved triggering, ability to develop custom readout firmware, etc. With this new hardware, it was possible to self-trigger or externally trigger the readout. In early studies, the self-trigger was identified as a significant technical challenge require additional resources and expertise to implement the firmware. In initial tests, defects in the Skiroc readout auxiliary board necessitated its return to the manufacturer for repair. The repaired electronics were received after the completion of this project, so further investigations were not possible. The results from this LDRD project hint at the significant technical capability presented by the use of these highly segmented silicon strips detectors and motivate continued investment to demonstrate a fully-realized radiation detection capability.

7.0 References

[1] M. P. Foxe, J. C. Hayes, M. F. Mayer, J. I. McIntyre, C. B. Sivals, and R. Suarez, "Characterization of a Commercial Silicon Beta Cell," Pacific Northwest National Laboratory (PNNL), Richland, WA (US)2016.

[2] M. P. Foxe and J. I. McIntyre, "Testing of the KRI-developed Silicon PIN Radioxenon Detector," Pacific Northwest National Laboratory (PNNL), Richland, WA (US)2015.

[3] <http://www.ti.com/product/AFE2256> (Texas Instruments, 2018)

[4] TI AFE2256 User Guide, available from vendor

Pacific Northwest National Laboratory

902 Battelle Boulevard
P.O. Box 999
Richland, WA 99354

1-888-375-PNNL (7665)

www.pnnl.gov